Acoustics of thunder: A quasilinear model for tortuous lightning[a)]

Herbert S. Ribner and Dipankar Roy[b)]
University of Toronto, Institute for Aerospace Studies, 4925 Dufferin Street, Downsview, Ontario, Canada M3H 5T6

(Received 11 January 1982; accepted for publication 23 August 1982)

An approximate quasilinear theory of thunder generation by tortuous lightning channels has been developed herein. It was applied to predict the major features of thunder, with details of the rumble and roll; these cannot be accounted for by current nonlinear treatments that exclude tortuosity. The waveform forecast is deterministic for a specific channel configuration and observer location: it is in effect *a mapping of the shape of lightning into the sound of thunder*. The lightning stroke is modeled as a tortuous line emitting N-shaped pressure waves from points all along its length. Although emitted simultaneously, they arrive sequentially according to distance: the received pressure signature is essentially a convolution of an N wave with a channel-shape function. Thus the thunder spectrum approximates a product form: an N-wave spectrum modulated by another due to channel tortuosity. In computer simulation a lightning channel was approximated as a zig-zag chain of straight segments; resolution was down to ~ 3 m to yield zero-crossing frequencies of order 200 Hz. Suitable 3-D shapes were generated, using appropriate deflection probabilities. The computer carried out the integration (here a summation) to produce the thunder pressure signature. With fast D/A, the output (a voltage) varies in real time; it was tape recorded for playback as *audible* synthetic thunder. Other calculations with "stylized" channel shapes showed how specific thunder features correlate one-to-one with geometric channel features. The emission from successive collinear segments was found to largely cancel, except as they approach perpendicularity to the sound rays: the latter case yields a focused thunderclap. Conversely, *the uncanceled emission from corners or kinks in a lightning channel was identified as a major element in thunder emission*. The corner effect accounts for the long duration (up to tens of seconds) of a real thunder signature compared with the single short thunderclap predicted for a long straight channel. The tortuous channel thunder predicted by the computer model was found to be compatible in (i) waveform appearance, (ii) spectral characteristics, and (iii) *audible* sound with real thunder (cf. bound-in soundsheet).

PACS numbers: 43.28.Fp, 92.60.Qx, 43.25.Vt

INTRODUCTION

Lightning and thunder are among the most dramatic of natural events, yet their understanding has long eluded us. In fact, the evolution from a supernatural to a rational explanation can be traced back for over 2000 years (see, e.g., Ref. 1 for a brief account). As recently as the late 1800's, four theories of thunder were in competition: the vacuum collapse theory, the electrolysis theory (explosive recombination of electrolyzed water), the steam expansion theory, and the ohmic heating theory (resistive heating and consequent expansion, due to heavy current discharge). The last, proposed by M. Hirn in 1888, is now accepted, being supported by a large body of consistent experimental data and theory.

The first serious mathematical theories of thunder did not emerge until well into the present century. The most credible of these (e.g., Refs. 4 and 5) incorporated realistic *nonlinear* gasdynamic effects and a very high temperature equation of state. But this rigor was somewhat offset by the simplifying assumption of axisymmetry: they modeled the lightning channel as a *vertical straight line*. The calculated pressure signature was in consequence but a single short thunderclap. This result is an applicable approximation only very close to an actual *tortuous* lightning channel.

The main theme of the present study is the delineation of the role of *tortuosity* of the lightning channel. This is demonstrated to be of major importance, accounting for the multiple claps and the rumble and roll that are characteristic of real thunder. (In the frequency domain it accounts for features of the spectrum.) This is ultimately exhibited via a computer model (cf. Ref. 1 and earlier work[2,3]).

In order to deal with tortuosity we are forced to depart from the nonlinear "rigorous" theory and go over to a quasilinear approximate theory; otherwise the loss of axisymmetry entails almost insuperable mathematical difficulties. The quasilinear approximation allows the thunder pressure–time signature at a point to be expressed in a formally simple fashion: it resembles a convolution integral. If the "crooked" lightning channel is approximated as a zig-zag chain of

[a)] Based on University of Toronto Ph.D. thesis by D. Roy[1] and earlier unpublished and published[2,3] work described therein, with both condensation and extension. In the process, the computer computations for three-dimensional lightning and its thunder have been replaced by new ones, with a wider range of parameters; an earlier error in the thunder calculations has been corrected. Prepared in part while senior author was on leave at NASA Langley Research Center, Hampton, VA 23665. Supersedes material presented at 10th International Congress on Acoustics, Sydney, Australia, July 1980; at 100th Meeting of the Acoustical Society of America, Los Angeles, November 1980; and at AIAA 7th Aeroacoustics Conference, Palo Alto, October 1981.

[b)] Now at Boeing Commercial Airplane Co., Noise Technology Research, P. O. Box 3707, MS-73-16, Seattle, WA 98124.

 0001-4966/82/121911-15$00.80

short, straight segments, the integral simplifies to a summation, convenient for a digital computer.

Owing to shortcomings of photographs, the channel geometry is likewise generated by computer. The procedure finally adopted is a random walk process in three dimensions, governed by appropriate deflection characteristics for the successive segments. This was developed to a point where the two-dimensional projections closely resembled photos of real lightning channels, and deflection histograms of two-dimensional simulations closely matched those of real channels.

Spectral comparisons of the computed and real thunder are made in the paper; however, they are far from decisive in assessing the degree of verisimilitude. Thus we also employ the human auditory system as a *pattern recognition* device.[6] To this end the computer output is fed through a real-time digital-to-analog converter into an amplifier-loudspeaker system to produce audible synthetic "thunder." Alternatively, the output of the D/A converter is tape recorded for future listening. It is this *audible* mode that demonstrates rather realistically the modeling of the sound of real thunder, displaying the characteristic claps, rumble, and roll.

Very similar notions on the role of tortuosity in thunder have been put forward independently and contemporaneously by Professor Few and his colleagues.[7–10] However, these were mainly qualitative and seemed also—in some of the reporting—to misread the precise role of the channel fine structure; they were not developed into a mathematical model of thunder. On the other hand, Dr. Few developed his ideas into a most ingenious procedure inverse to ours for real thunder: he and his colleagues showed how to reconstruct a lightning channel configuration from the measured short-term (1/4 to 1/2 s) thunder pressure correlations between microphone pairs in an array. This technique has been developed into a powerful diagnostic tool for lightning research (e.g., Ref. 11).

The procedure of Few *et al.*, and ours are complementary but not equivalent: we require some 2000 points to specify a 6-km lightning channel in sufficient detail to delineate the emitted thunder waveform, hence the sound; their reconstruction falls far short of this, apparently yielding no more than 75 points.[11,12] (The time average needed to obtain a correlation is effectively a spatial average over emitting points along the channel.)[13]

Independent studies in several respects *parallel* to ours have been carried out by LeVine and Meneghini[14,15] in connection with the electromagnetic radiation from lightning (sferics). Both sets of studies employed computer algorithms to generate three-dimensional lightning channels as a random walk or Monte Carlo procedure. And both emphasized the role of *tortuosity* on the relevant signature (pressure or electromagnetic) and its spectrum.

I. QUASILINEAR LIGHTNING→THUNDER MODEL

A. Thunder as superposition of *N* waves

Near thunder reflects its explosive origin in being strongly nonlinear in its early evolution. Mathematically this can be dealt with in an axisymmetric format,[4,5] yielding

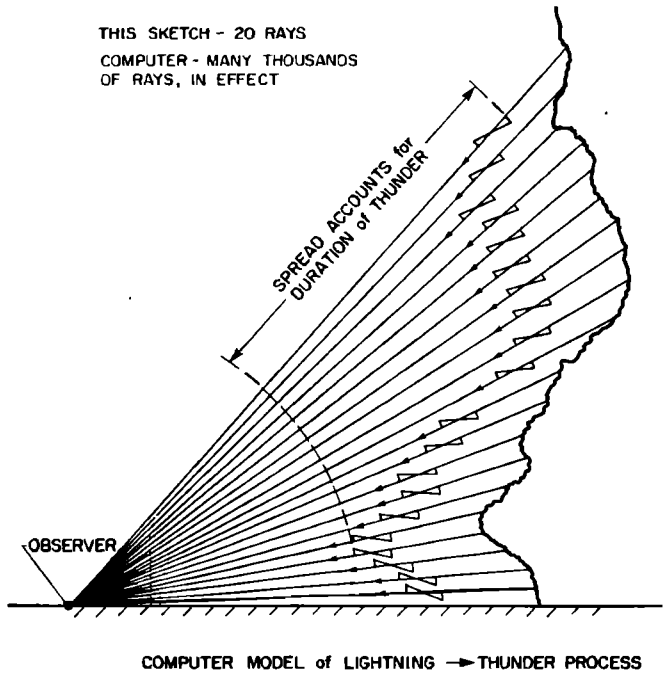

FIG. 1. Quasilinear lightning→thunder model: each point of channel emits explosive pressure wave that evolves nonlinearly—and independently—into an *N* wave.

an expanding cylindrical shock wave. When the shock radius exceeds the length of an essentially straight section of channel, the axisymmetry breaks down.[7] Accommodation of the further nonlinear evolution to the channel tortuosity is beyond the present state of the art. In the present heuristic theory we have replaced this early evolution by an approximation that permits ready application to channel tortuosity.

The theory is as follows[1–3]: a lightning stroke of specified shape is modeled as a line distribution of strong impulsive point sources (point explosions). A sonic boomlike pressure wave is assumed to evolve spherically by nonlinear propagation from each point, *independently* (Fig. 1): the perturbation pressure $p(t)$ is shaped like the letter "N." The independence approximation is a key element: it implies that the *N* waves from each emission point may be added *linearly* (integrated) at any reception point that is not too close (not within the nonlinear evolution distance). This summation yields the pressure–time signature of the local thunder. (A similar notion was put forth independently by Wright and Medendorp[16] to model the sound emission from a spark, the channel being considered straight and short.)

The *N* wave of pressure that evolves nonlinearly from the element ds of the channel at distance r from the observer is taken to have an asymptotic form[17] $(A/r)N(ct-r)ds$. The amplitude A and duration $2T$ are governed by the energy released per unit length in the lightning discharge (cf., Ref. 1).[18] Summing over the entire tortuous lightning channel, s being measured upward from the base, gives

$$p(t)=\int_{\text{channel}} N(ct-r)\left(\frac{A}{r}\right)ds \tag{1}$$

as the pressure signature received by the observer. Since r is a function of s, this *maps the shape of the lightning channel in*

space into the shape of the pressure signature in time. The mapped signature depends also (in a somewhat hidden fashion) on the N-wave character of the overlapping building elements.

Mathematically, when $2T$ is held constant, Eq. (1) is effectively a convolution integral: it is thrown into a more recognizable form in the later section on spectra. As a convolution integral it displays in simplest fashion the dual dependence on lightning channel geometry (in space) and N-wave geometry (in time or space).

Analytical integration of (1) becomes feasible when the lightning channel is approximated as a zig-zag chain of straight segments: given the amplitude A, the integration can be carried out[16] to yield the pressure signature radiated from any individual line segment in terms of appropriate distance/orientation parameters. This is a *computer building block for thunder*: the formula can be programmed into a computer along with the spatial configuration of a given lightning channel. Then, for a specified reception point, the computer can sum the signatures from all the lightning segments, keeping track of their respective arrival times, to produce the extended pressure–time history of the thunder signature.

Such a pressure calculation is normally output from the computer as an x–y plot. However, if the computer digital/analog (D/A) converter is fast enough for real-time conversion, an interesting possibility emerges: the signal (a voltage) can be introduced into an amplifer–loudspeaker system to produce *audible* synthetic thunder.

B. Computer building blocks: Wright–Medendorp waves

Evaluation of one of these computer building blocks, the emission from a single line segment, follows from the discussion preceding Eq. (1): an element dz of a lightning segment $2l$ "emits"[17] an N wave with amplitude $A\,dz/r'$ at distance r'. This multiplies a shape factor which may be written

$$N(ct') = -\left[\frac{t'}{T}\right]\cdot\begin{cases}1 & |[\,]|\leqslant 1\\ 0 & |[\,]|>1\end{cases} \tag{2}$$

at distances near r'. Travel of the wave along rays r' at the speed of sound c is implied by replacement of t' by $t - r'/c$. Summing all these N waves emitted from the lightning segment $2l$ gives the sound pressure signature therefrom as[18]

$$p(t,r) = A\int_{-l}^{l}\frac{N(ct-r')}{r'}\,ds, \tag{3}$$

where r' is the distance from the observer to dz and r the distance to the midpoint of the segment.

The vector $\mathbf{r}$ makes an angle ϕ with the normal to the segment. At large distances (farfield) the rays $\mathbf{r}$ and $\mathbf{r}'$ are nearly parallel. A sufficient approximation is

$$r' \cong r - z\sin\phi \tag{4}$$

in the numerator ($\sim$ phase of N wave) and $r' = r$ in the denominator ($\sim$ amplitude). With these approximations Wright and Medendorp[16] carried out the integration of (2). The integrated pressure is expressed in terms of the nondimensional parameters

$$\tau = \frac{ct-r}{l};\quad \psi = \frac{cT}{l};\quad B = \frac{Al^2}{2rcT}, \tag{5}$$

involving the period $2T$ and amplitude A of the constituent N waves, the length $2l$ of the segment, and the distance r of the observer; c is the speed of sound.

The pressure signature (*Wright–Medendorp wave*) emitted by a lightning segment at angle ϕ to its normal comes out to be

$$p = p_+ + p_-. \tag{6a}$$

This consists of a positive parabolic pulse

$$p_+ = B\left[\frac{\psi^2 - (\tau + |\sin\phi\,|)^2}{|\sin\phi\,|}\right]\cdot\begin{cases}1 & \text{when } [\,]>0\\ 0 & \text{when } [\,]\leqslant 0\end{cases} \tag{6b}$$

plus a negative parabolic pulse

$$p_- = -B\left[\frac{\psi^2 - (\tau - |\sin\phi\,|)^2}{|\sin\phi\,|}\right]\cdot\begin{cases}1 & \text{when } [\,]>0\\ 0 & \text{when } [\,]\leqslant 0\end{cases}. \tag{6c}$$

For rays at sufficient inclinations $|\phi\,|$ to segments that are not too short ($\psi < 1$) the p_+ and p_- are quite distinct: the signature consists of separate $+$ and $-$ parabolic pressure pulses with a *quiet* space between—there is complete cancellation of the superposed N waves (Fig. 2, left-hand side). At smaller inclinations ($|\sin\phi\,| < \psi$) the $+$ and $-$ pulses overlap. The summed pressure in the region of overlap is rectilinear with time:

This can be seen by direct addition of (6b) and (6c), the result being $-4B\tau$. [The singularity in (6b) and (6c) may cause difficulty in computer implementation near $\phi = 0$: for a more elaborate alternative formulation that avoids this, see Refs. 1 or 16.]

The parameter ψ in Fig. 2 ($\sim$ N-wave duration) was chosen as 0.293 for best match at $\phi = 65°$ with an experimental waveform[16] for a spark (right-hand side). The general agreement with the theoretical waveform—two pulses separated by a long flat spot—is seen to be quite good. However,

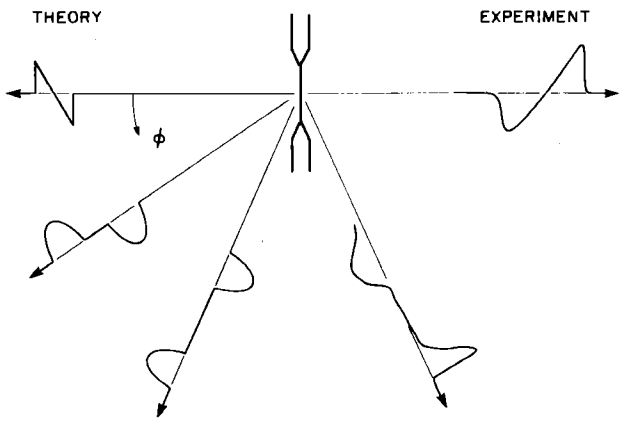

FIG. 2. Sound radiation from short channel segment versus ray angle (cf., also Fig. 5). Theoretical waveforms (left-hand side, normalized to uniform amplitude) result from summed N waves. N-wave duration ($\psi = 0.293$) is chosen for best match with experiment (right-hand side) at $\phi = 65°$. At $\phi = 0$ the difference in length is attributed to nonlinear stretching (experiment). Adapted from Wright and Medendorp,[16] in the context of sound emission from sparks.

the front pulse has been distorted by nonlinear steepening into almost half an N wave. At $\phi = 0$ the predicted N-wave shape is found experimentally, but stretched—again by nonlinear effects—to over twice the duration. In a series of measurements[16] with 0.5- and 1.0-cm sparks, the theoretical variation of peak amplitude with angle ϕ was quantitatively confirmed experimentally, except at small angles (region of pulse overlap); here wave stretching markedly reduced the amplitude. Less accurately, the predicted trend with ϕ of the length of the flat spot was found.

C. Effects of refraction

It is implicit in the earlier analysis that the *sound rays are straight*, and they coincide with the vectors that fan out from the observer point to points along the lightning channel. However, owing to gradients in atmospheric temperature, as well as wind, the *sound rays will normally be curved* by refraction. The radius of curvature is, however, very large—typically over 80 km in the absence of wind (reduced to some 55 km in thunderstorms)—so that the rays are very nearly straight over the distances of interest. Hence our assumption of rectilinearity should entail little error for distances up to 5 km or so: a given lightning channel with curved rays is mapped thereby into a slightly shifted, distorted channel that is virtually equivalent acoustically. However, the assumption could be relaxed at a cost of greater complexity in the computer program.

The generally decreasing speed of sound with altitude will, in the absence of countervailing winds, cause the rays to curve upward. A ray tangentially reaching an observer on the ground will thus meet the channel at some distance above the ground. Typically this might be of order 35 m for an observer distance of 2 km. Rays emitted from points of the channel below this height cannot reach him: they will graze the ground tangentially at a closer distance and pass over his head to create a sound shadow.

The ray curvature being roughly circular, there is roughly a quadratic relationship: the 35-m shadowed emission zone grows to about 5.5 km—a typical lightning channel height—as 2 km grows to 25 km. This refraction-created shadow effect (together with atmospheric and ground attenuation) helps explain why thunder from cloud-to-ground strokes cannot ordinarily be heard at distances from the stroke exceeding 25 km or so.

The edge of the sound shadow is not sharp: some sound can penetrate by diffraction, not accounted for in our ray acoustics. This may be manifested as a weak precursor to the stronger ray acoustics thunder. The expectation is a low-frequency rumble leading the initial thunderclap. Based on path length, the lead time should range from a few milliseconds at the smaller observer distances (<4 km, say) to roughly half a second at 15 km. By contrast, the onset of our present computer generated thunder—which does not allow for curved rays and diffraction—is unrealistically abrupt. Some guidance as to a method for calculating the diffraction may be found in a paper by Onyeonwu[19]: it deals with the analogous problem of refractive cutoff of a sonic boom. However, it takes no account of the important effects of ground absorption in attenuating the high frequencies.[20]

The ray acoustics discussion refers to gross average refraction effects in the atmosphere. Stratified or even localized wind gradients and temperature inversions can modify these greatly: in particular there can be channeling of sound and focusing and defocusing of sound rays. (The latter is also an aspect of scattering by the large eddies of atmospheric turbulence.[21]) When such weather features are significant the simple assumption of ray rectilinearity entails considerable error. It is then necessary[12] to incorporate temperature and wind profiles into ray-tracing programs.

II. "STYLIZED" LIGHTNING

We have noted that a fluid-dynamically "rigorous" approach to thunder generation is practicable in the special case of an axisymmetric channel.[4,5] A key question was whether the present quasi-linear theory is compatible in its gross features. Thus the comparison required the application of our model to the case of a rectilinear stroke. The calculations (see below) were quite informative, and they led the authors to try several other cases of "regularized" or "stylized" lightning. The results allowed some general conclusions relating specific features of thunder to features of the lightning geometry on a one-to-one basis.

A. Emission from long rectilinear channel

A 6-km vertical lightning channel is considered to be built up from 3-m segments. The integrated sound emission from a given segment in a given direction is a Wright–Medendorp wave,[16] as discussed earlier (Fig. 2). The individual W–M waves are shown superposed in the top section of Fig. 3: they are based on a duration $2T = 5$ ms for the constituent N waves and an observer distance of 800 m. The bottom section shows the resultant pressure–time signature from summing these overlapping waves. This is a *single "thunderclap"* of duration about twice the basic N-wave length. Comparison with the superposed waves of the top section of the figure is illuminating: it shows strong mutual *reinforcement* for the earliest 20 to 30 waves, quickly progressing to almost complete *cancellation* among all the later waves—those from higher up the channel. Thus, at this distance, only the *bottom* 60 *to* 90 *m* of the 6-km stroke really contribute to the thunderclap!

For comparison, Fig. 4 shows rigorously calculated thunderclap waveforms obtained by Plooster.[22] These apply at distances less than 10 m or so, and nonlinear theory predicts eventual stretching/distortion into N waves at large distances. The signature of Fig. 3 differs significantly from all of these, including the N wave. However, the gross feature of a single thunderclap of credible duration—given a defensible estimate of the N-wave duration—is reproduced.

B. Cancellation and noncancellation: Corner effect

The cited wave reinforcements in Fig. 3 are associated with W–M waves from the lowest segments of the channel: these move along rays that are inclined at small angles ϕ to the segment normal (cf., Fig. 2). The wave cancellation, on the other hand, is associated with W–M waves from higher segments: their rays make larger angles with the segment

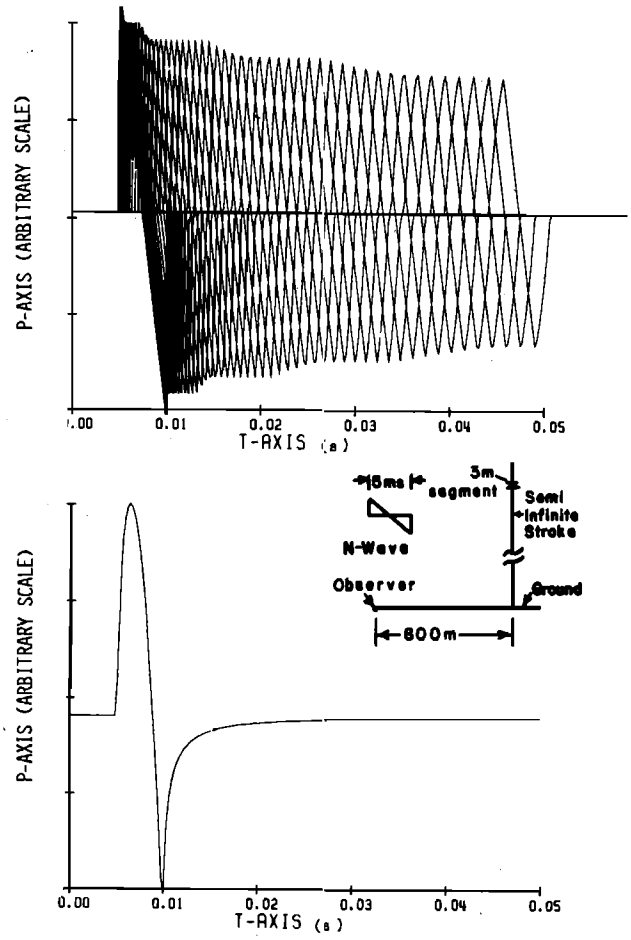

FIG. 3. Semi-infinite stroke, quasi-linear theory for *farfield* (800 m): superposition of W–M waves from 3-m segments (top) builds up into thunderclap (bottom).

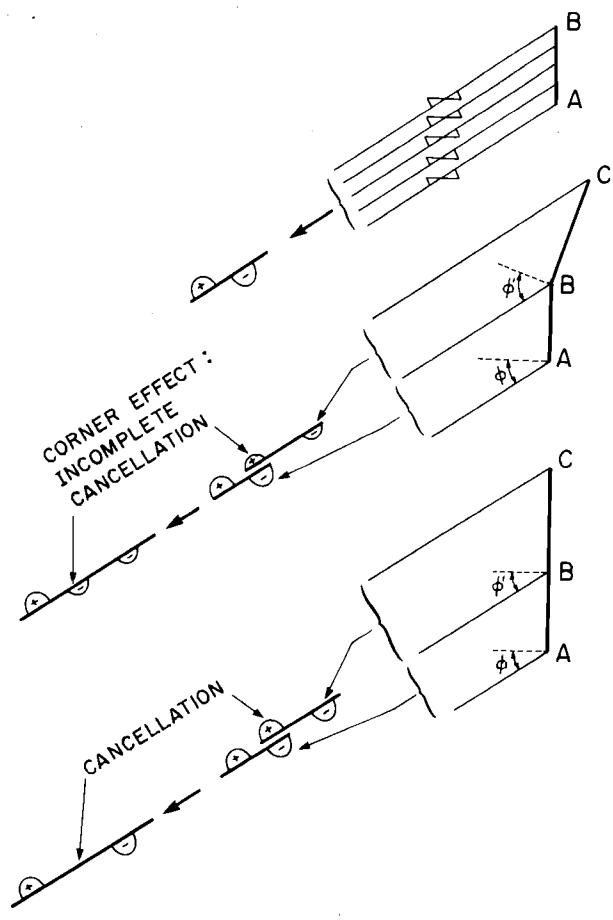

FIG. 5. Illustration of incomplete cancellation of W–M waves at a junction: the *corner effect*. Thus unlike a straight channel, a crooked channel *emits from all along its length*, at the zig-zag corners; this accounts for the long duration of real thunder, as well as details of its signature.

normal. Note the progression in Fig. 2 from quasi-N waves at small ϕ to separated parabolic pulses at larger ϕ. The waves emanating from higher up the channel—not shown in Fig. 3—will have this parabolic shape.

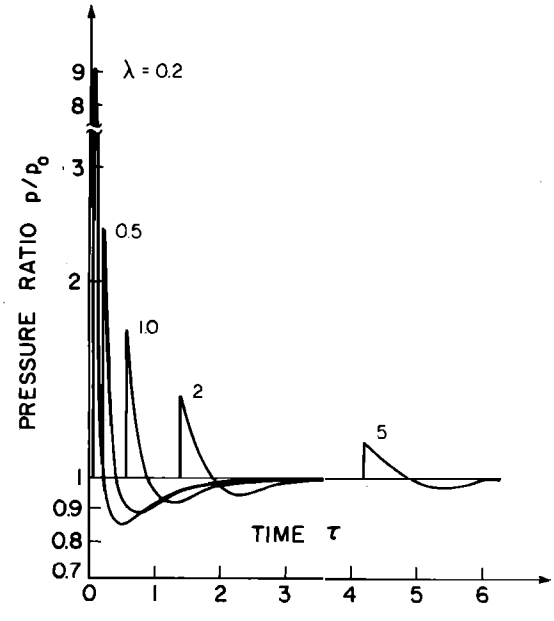

FIG. 4. Semi-infinite stroke, rigorous *nearfield* calculations (up to ~10 m) after Plooster.[22]

In the parabolic regime the cancellation effect for the sound emission from the abutting ends of a pair of collinear segments is clearly evident. This is very graphically shown in the bottom sketch of Fig. 5. However, incomplete cancellation will occur when successive segments are *angled* to one another. The middle sketch, Fig. 5, shows a net uncanceled emission from the junction: this is the *corner effect*.

C. Emission from localized kink

The *corner effect* accounts for the extra localized sound emission from a "kink" in an otherwise straight channel: a local spoilage of the wave cancellation. A rectilinear lightning stroke with a kink at the 45th and 46th 3-m segments is modeled in Fig. 6. There is now a second thunderclap some 40 ms after the first one: the *6-m kink emits a pulse of one-fifth the amplitude of the basic clap from the 6000-m straight channel.*

D. Emission from stylized channel

The inset diagram of Fig. 7 shows a regularized or stylized lightning channel built up of 3-m straight segments. The observer is at a distance of 600 m. Segments 1 to 44 are collinear and vertical: their emission accounts for the *first*

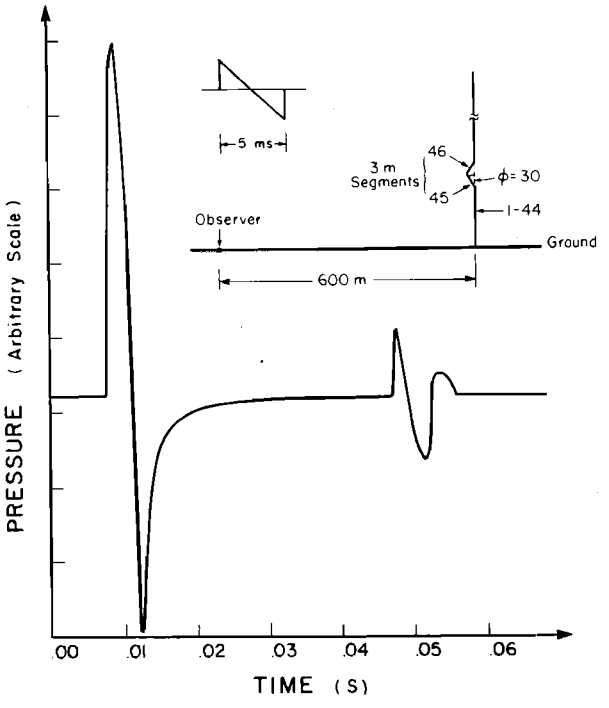

FIG. 6. Local "kink" in an otherwise straight stroke generates a weak second thunderclap.

thunderclap in the pressure signature shown on the figure. This thunderclap is the same as that for the long (6 km) vertical channel of Fig. 3.

The figure shows an *even stronger second thunderclap.* This is traceable to a *focusing effect* of segments 45–54: these are arranged tangent to a circular arc centered on the observer. The perpendicular ray-segment orientation ($\phi = 0$) yields W–M waves (Fig. 2) of almost pure N wave form. The segments being equidistant from the observer, the waves all arrive in phase to provide a tenfold focusing enhancement.

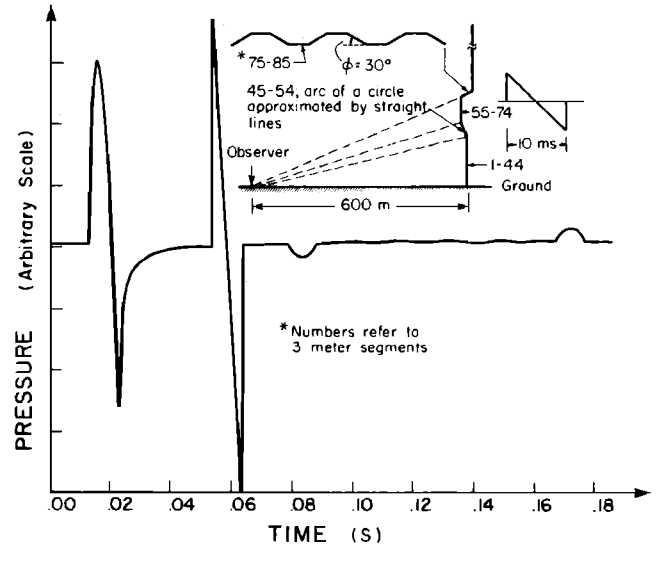

FIG. 7. Pressure signature received 600 m from a "stylized" lightning stroke. Segments 45–54 normal to sound rays yield focused *thunderclap* (at $t \simeq 0.06$ s). Segments 75–85 lying more or less along a sound ray yield a weak *rumble* ($t = 0.09$ to 0.17 s).

Segments 55–74 are again vertical and contribute merely a small termination pulse (negative parabola).

Segments 75–85 lie essentially along the *ray* from the observer to 74: they are inclined 30° from one another to form a roughly sinusoidal modulation of this ray. The corresponding section of the thunder pressure signature seems very close to a sinusoid, but of very low amplitude. We interpret this as a *rumble.*

E. Inferences for real thunder

In summary, the stylized channel calculations show that: (i) channel sections essentially *normal* to the ray to the observer provide approximate focusing to yield strong *thunderclaps*: the longer the section and the more nearly it conforms to a circular arc, the stronger the thunderclap; (ii) channel sections lying more or less along the ray to the observer yield weak *rumbles*; (iii) the myriad *corners* or kinks along a crooked channel emit individual pulses.

Essentially the same conclusions as (i) and (ii) have been drawn by Few,[10] on the basis of qualitative arguments. He replaces *corner* emission (iii), however, by a shock-expansion wave from each zig-zag segment. Taken together, these constitute his "string-of-pearls" model[7] of thunder emission. This very apt descriptor would fit either model.

F. Calibration of thunder parameters

The amplitude A and duration $2T$ of the basic N waves of our model remain to be specified in terms of the lightning channel strength: the energy E_l released per unit length. It is suggested in Ref. 1 that this can be done by forcing an approximate match of calculations via the quasi-linear model with those of a published "rigorous" nonlinear model (e.g., Refs. 4 and 5). These are applied to the emission from a long, rectilinear, vertical chamber, since the rigorous models cannot cope with tortuosity.

That scenario, however, implies cylindrical wave propagation all the way. However, as pointed out by Few,[7] for tortuous lightning a transition to spherical propagation occurs a few meters from the channel. Thus the match is of dubious applicability for quantizing a real thunder signature. Instead we tentatively advocate a more empirical approach: the N-wave duration is chosen for best match of the spectral peak frequencies (see later) of computer thunder and real thunder, and the amplitude A for best match of typical signature amplitudes at comparable distances from the stroke. These choices refer to the dominant stroke in a multistroke flash: the others are scaled therefrom as described under Table I.

III. TORTUOUS LIGHTNING

A. Fine structure

Considerations of the average zero-crossing frequencies in thunder dictate the fine structure of the lightning channel: how short the zig-zag segments must be. Assume a channel of average height, ~5 km, terminating vertically above the base. An observer at, say, 3 km from the base is some 5.8 km from the top end. At 343 m/s the difference in acoustic travel times (duration of the thunder) is 8.2 s. Since typical thunder spectra contain strong (upward sense) zero-crossing frequen-

TABLE I. Parameters of selected signatures of computer-generated thunder.

Thunder Signature	Lightning Stroke	N-Wave Duration (ms) $2T_0$	N-Wave Amplitude A	Observer Position (km) x(o)	y(o)	z(o)	No. of Strokes	Relative dB of Highest Peak
$p_1(t)$	L_1	10	1.0	-7	0	0	Single	0.59
$p_2(t)$	L_1	5	1.0	0	-5	0	Single	-1.20
$p_3(t)$	L_2	2.5	1.0	-3	0	0	Single	1.44
$p_4(t)$	L_2	10.	1.0	0	-6	0	Single	1.51
$p_5(t)$	L_1	7.	.6	-7	0	0	Single	-7.77
$p_6(t)$	L_1	5	.35	-7	0	0	Single	-16.08
$p_7(t)$	$=p_1(t) + p_5$ (t-.05 sec) + p_6 (t-.12 sec)						Triple	2.52
$p_8(t)$	L_1	3.5	.6	0	-5	0	Single	-8.25
$p_9(t)$	L_1	2.5	.35	0	-5	0	Single	-16.14
$p_{10}(t)$	$=p_2(t) + p_8$ (t-.06 sec) + p_8 (t-.12 sec)						Triple	-.90
$p_{11}(t)$	L_2	1.75	.6	-3	0	0	Single	-4.21
$p_{12}(t)$	L_2	1.25	.35	-3	0	0	Single	-14.33
$p_{13}(t)$	$= p_3(t) + p_{11}$ (t-.07 sec) + p_{12} (t-.12 sec)						Triple	-7.3
$p_{14}(t)$	L_2	7	.6	0	-6	0	Single	-4.64
$p_{15}(t)$	L_2	5	.35	0	-6	0	Single	-10.26
$p_{16}(t)$	$= p_4(t) + p_{14}$ (t-.06 sec) + p_{15} (t-.12 sec)						Triple	0.79
$p_{27}(t)$	L_2	2.5	.35	0	-0.18	0	Single	8.88

For triple-stroke lightning flashes an energy (per unit length) sequence 1:½:¼ is not untypical: these underlie the choices for relative N-wave amplitude A and duration $2T_0$ in the Table. T_0 has been taken to scale with (energy)$^{1/2}$ and A with (energy)$^{3/4}$. (Our conceptual modelling of the process - still tentative - has changed, and we would now scale A with (energy)$^{1/2}$; this follows from a variant of the thinking of Few[7], with transition from cylindrical to spherical wave propagation considered to occur at approximately one relaxation radius[7] from the channel.) The individual thunder sigratures, $p_i(t)$, as originally calculated, differ markedly in amplitude (last column) as A, $2T_0$, and observer distance vary. However, in the digital/analog conversion they are rescaled in the computer to comparable peak amplitude. Thus relative loudness levels on the soundsheet are fairly comparable, except as indicated in a later reference note.

cies to over 200 Hz, at least 1640 cycles will be recorded. Now the Wright–Medendorp (W–M) wave emitted from a single segment contributes only a single upward zero crossing. Thus some 1640 segments (angled to provide uncanceled emission from the corners) are needed in order to generate the required 200 Hz. This subdivides the 5000-m channel into angled segments averaging approximately 3 m in length.

A typical photograph of a cloud-to-ground lightning channel can be resolved, however, only down to 40- to 60-m segments. Thus the photograph falls far short of exhibiting the fine structure that our acoustic considerations (supported by limited telephoto data[9,10]) tell us must be present. In our earlier work we supplemented photographs with an artificial computer-generated fine structure. It was with such channel shapes that the first *audible* computer-generated thunder was obtained.[2,3]

The shortcomings of the hybrid photograph–computer-generated channels are elaborated in Ref. 1; they became increasingly apparent with the passage of time. It was finally decided to go over to a fully computer-generated channel geometry, for internal consistency and other reasons. A single set of statistics for the zig-zag deflections would govern both the fine and gross structure, ultimately in three dimensions.

B. Random walk: Two-dimensional statistics

The earliest choices for the deflection statistics led to unrealistic lightning channel shapes. A later encounter with Hill's work[23] suggested a Gaussian probability density

$$p(\Delta\theta) = a \exp[-(\Delta\theta^2/\Delta\theta_m^2)] \quad (7)$$

for the deflection $\Delta\theta$ of one segment from the next. This generated more realistic looking shapes, except for a tendency of the channel to wander far away from the vertical and even turn downward. It was clear that a *bias toward the vertical* was required: this was supplied as a term θ/N in the modified probability

$$p(\Delta\theta) = a \exp[-(\Delta\theta + \theta/N)^2/\Delta\theta_m^2)]. \quad (8)$$

In conjunction with this the segments were taken to have a Poisson distribution in length

$$p\left(\frac{l}{l_p}\right) = b\left(\frac{l}{l_p}\right)\exp\left(\frac{-l}{l_p}\right). \quad (9)$$

The general channel contours so developed were not too unrealistic, but features of the order 60–80 m were found to be too irregular. Variations of $\Delta\theta_m$ and of N (which interact) did not succeed in generating sufficiently realistic shapes. Finally it was decided to incorporate *memory smoothing*. To this end the probability density was modified to the form

$$p(\theta_n - \bar{\theta}_{n-1}) = a \exp[-(\theta_n - \bar{\theta}_{n-1} + \bar{\theta}_{n-1}/N)^2/\Delta\theta_m^2], \quad (10)$$

wherein

$$\bar{\theta}_{n-1} = \frac{1}{k}\sum_{n-1-k}^{n-1}\theta_i.$$

Here $\bar{\theta}_{n-1}$ is the average angle to the vertical of the k segments previous to the segment at angle θ_n. The rationale is a "hand-waving" physical argument: the electric field governing the propagation of the stepped leader is presumably influenced by the trend (average direction) of the last k steps, rather than by just the last step alone.

C. Computed channels, tortuosity histograms, and thunder

It was found that the *memory smoothing* could reduce the channel fine structure irregularity to realistic levels. But the parameters $\Delta\theta_m$, k, and N interact, so that much computer experimentation was required.[1] The most realistic computer generated channel in *two dimensions*—using both Eqs. (9) and (10)—is shown in Fig. 8 (mean segment length 3 m; vertical bias $N = 20$; $k = 4$; $\Delta\theta_m = 30°$). This shows the entire 4.6-km channel, and the fine structure is not visible [for that, see Fig. 56(b) of Ref. 1]. The degree of resemblance to real lightning may be judged from comparison with Fig. 9, after Garrett (in article by Few[10]).

In the manner of R. D. Hill,[23] using photographs of ten *real* lightning channels, we have developed histograms of the deflection probabilities of successive sections, estimated to be of order 60 m, from one another: these statistically describe the channel "crookedness." We have done the same for 60-m sections of the *computer generated* channel of Fig. 8. The comparative tortuosity histograms, shown in Fig. 10, are seen to agree remarkably well. Thus both visual and statistical tests seem to affirm the credibility of our two-dimensional random walk model of tortuous (but unbranched) lightning.

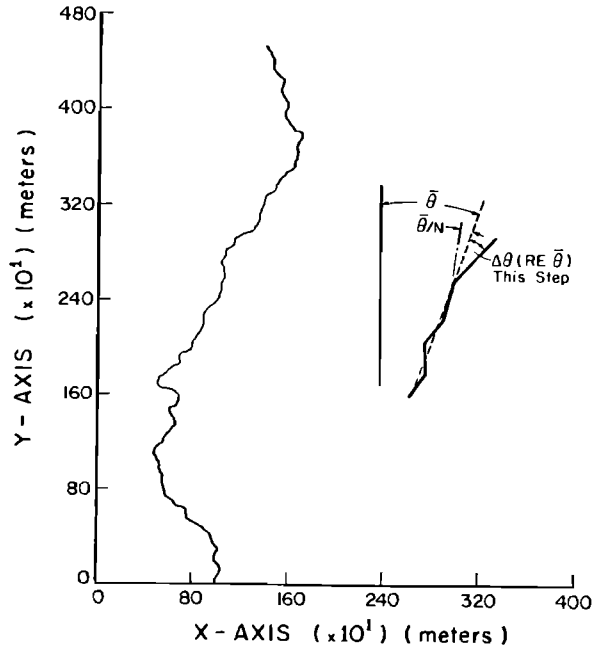

FIG. 8. Two-dimensional computer-generated "lightning" channel.

Reference 1 details how the lightning–thunder algorithm discussed earlier was applied to such channels to yield *audible* computer-generated thunder (see also Refs. 2 and 3).

FIG. 9. Photograph of lightning channels near Tucson, Arizona, made by Henry B. Garrett. (Reproduced from Scientific American, article by Few.[10])

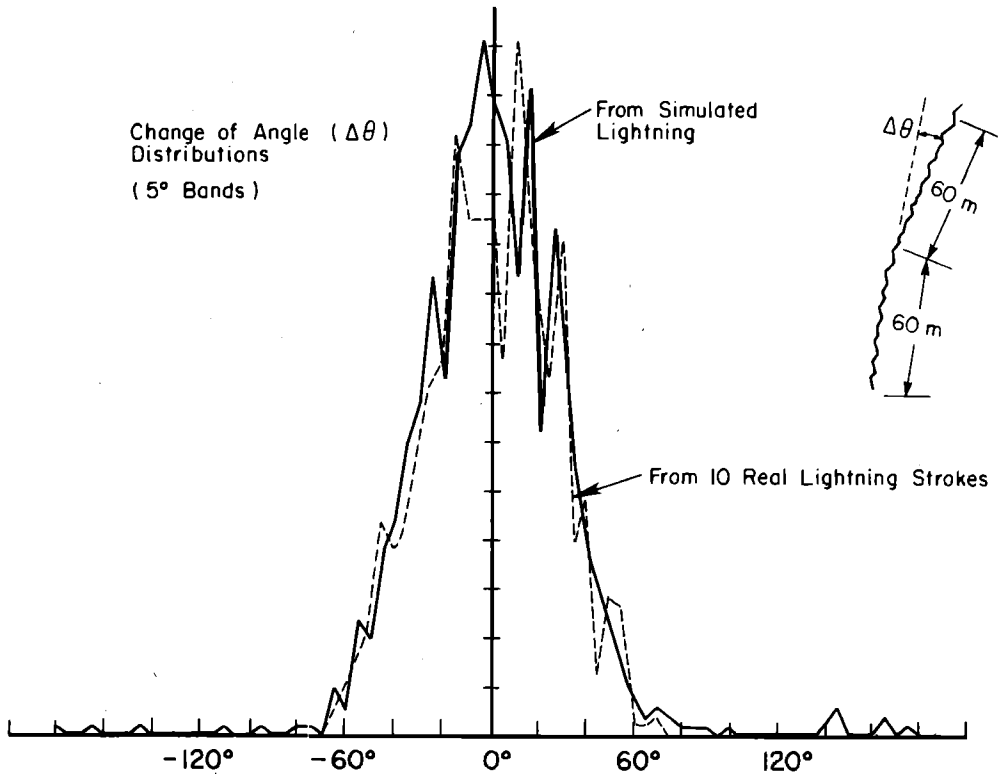

FIG. 10. Comparative histograms describing lightning channel tortuosity.

D. Random walk: Three-dimensional statistics

In hindsight, our work with two-dimensional (2-D) channels was, even qualitatively, an oversimplification. It was rather belatedly realized that whereas the 2-D probability density is a Gaussian in the 2-D segment deflection $\Delta\theta$, the 3-D probability density is $\sin\Theta$ times a Gaussian in the 3-D polar deflection Θ. Thus whereas in 2 D the deflection of highest probability is *zero*, in 3 D the deflection of highest probability is a *finite value*. This implies a qualitative difference in the thunder that would be generated.

More specifically, the deflection angle governs the *corner effect* that dominates the emission from the channel fine structure: *this emission constitutes a sort of high-frequency pattern that is modulated by the gross structure of the channel.* Suppose we compare the thunder emitted from a 3-D channel with that emitted from a 2-D channel of the same energy per unit length whose shape is the projection of the former on a vertical plane. It follows that the high-frequency pattern of the 3-D channel will be the stronger, among other differences.

Here again, on the role of the fine structure, our ideas, developed independently of Few,[7-10] have been rather parallel on the broad features, although differing on detail.

We proceed now to establish the 3-D statistics governing the relative deflections of successive lightning segments in a zig-zag chain. Let **a** be the vector sum of k segments (to provide *memory smoothing*, as in the 2-D case) lying at an angle θ to the vertical. From the end of **a** erect a unit vector **b** inclined at an angle θ/N closer to the vertical (viz., angle between **a** and **b** is θ/N) (this provides a *bias toward the vertical*, as in the 2-D case). Imagine that the next segment is inclined by some polar angle Θ to **b**; the assumption is that this segment can be anywhere on a cone of semiangle Θ, with **b** an axis, with equal probability.

More specifically, the probability that the segment terminates on a sphere within solid angle $d\Omega = \sin\Theta\, d\Theta\, d\psi''$ is taken to have the form

$$p(\Theta)\,p(\psi'')d\Theta\,d\psi'' = a\sin\Theta\exp(-\Theta^2/\Delta\theta_m{}^2)d\Theta\,d\psi''/2\pi. \tag{11}$$

This factors into a uniform probability in ψ'', an azimuth angle defining the position around the cone,

$$p(\psi'') = 1/2\pi \tag{12}$$

and a Gaussian probability in the polar angle

$$p(\Theta) = a\sin\Theta\exp[-\Theta^2/\Delta\theta_m^2] \tag{13}$$

exhibiting the extra factor $\sin\Theta$ arising from the solid angle $d\Omega$, compared with the two-dimensional case.

E. Random walk: Three-dimensional computed channels

The deflection probabilities (11) to (13), together with the Poisson segment length distribution (9), were implemented to generate 3-D "lightning" channels on the computer. The statistical parameters were varied until the x–y plots of their 2-D projections appeared most realistic. The linear *vertical bias* $\bar{\theta}/N$ that yielded good verisimilitude for the earlier 2-D channels was not fully satisfactory in the 3-D case. Best realism was found on replacing this with a quadratic form $0.0008\,\bar{\theta}^2$, with certain choices for the other parameters: $\Delta\theta_m = 25°$ (governing the rms deflection) and five-segment averaging for the $\bar{\theta}$, with the segments l_i averaging 3 m in length as before.

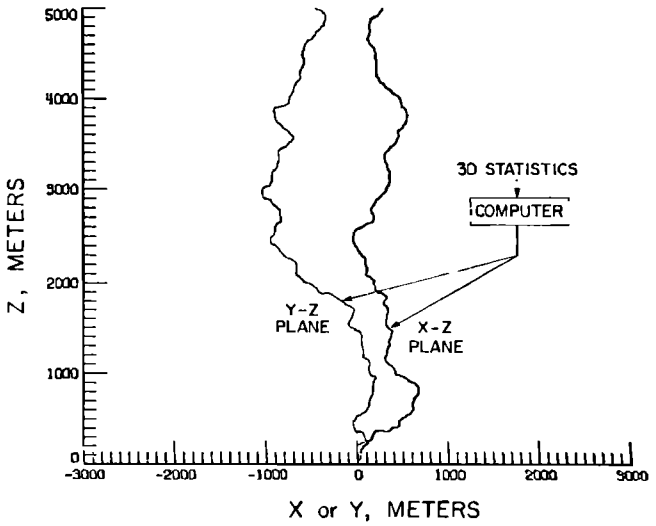

FIG. 11. Orthogonal projections of three-dimensional computer-generated "lightning" channel, L_2.

Orthogonal projections of a particular computer-generated channel obtained with these "best" statistics are shown in Fig. 11. This channel, designated L_2, is one of two utilized in the present paper. Another channel, designated L_1, with the same statistics, was generated via a different set of random numbers.

IV. THUNDER FROM TORTUOUS LIGHTNING

A. Thunder signatures by computer

The thunder algorithm described earlier was applied to the 3-D lightning channels L_1 and L_2. In calculating the emission—a Wright–Medendorp wave[16]—from a given short channel segment, the differential nonlinear stretching of the constituent N waves was ignored. But stretching was allowed for in the amplitude and duration parameters of the separate W–M waves from channel segments with centers at differing distances r_i from the observer. Thus the half-duration T was considered to stretch $\sim[\ln(r/a)]^{1/2}$, an asymptotic law (e.g., Ref. 24), implying an inverse change in amplitude. Correspondingly, two of the defining parameters for the W–M waves, Eq. (5), were replaced by modified values

$$\psi_i = \frac{cT_0}{l}\left(\frac{\ln(r_0/a)}{\ln(r_i/a)}\right)^{1/2}; \quad B_i = \frac{Al^2}{2r_icT_0}\left(\frac{\ln(r_0/a)}{\ln(r_i/a)}\right),$$

specific to the ith segment. In the calculations a and r_0 were taken as 10 and 1000 m, respectively. The duration $2T_0$ at 1000 m was given various values (Table I).

The differential stretch between N waves arriving along the shortest and longest rays provides the extreme of significance for the thunder signature. This is rather small: e.g., N waves that have traveled 3.6 km are figured to be only 20% longer than those that have traveled 0.6 km. (A more accurate law, due to Gottlieb,[25] proportions the stretch to $[1 + \text{const}\ \ln(r/a)]^{1/2}$. With this law, using the appropriate constant, the differential stretch is reduced to 15%.)

A 0.1-s segment of a thunder pressure signature calculated in this fashion is shown in Fig. 12. This signature is identified as p_8 in Table I, which details the parameters and observer location. At the top of the figure are shown superposed Wright–Medendorp waves [Eq. (6)] from the individual channel segments (averaging 3 m); at the bottom is shown the resultant pressure–time history: the thunder pressure signature.

Figure 12 refers to the thunder from a single stroke. Typically, however, a lightning flash consists of several successive strokes, of order 60 ms apart in time, along the

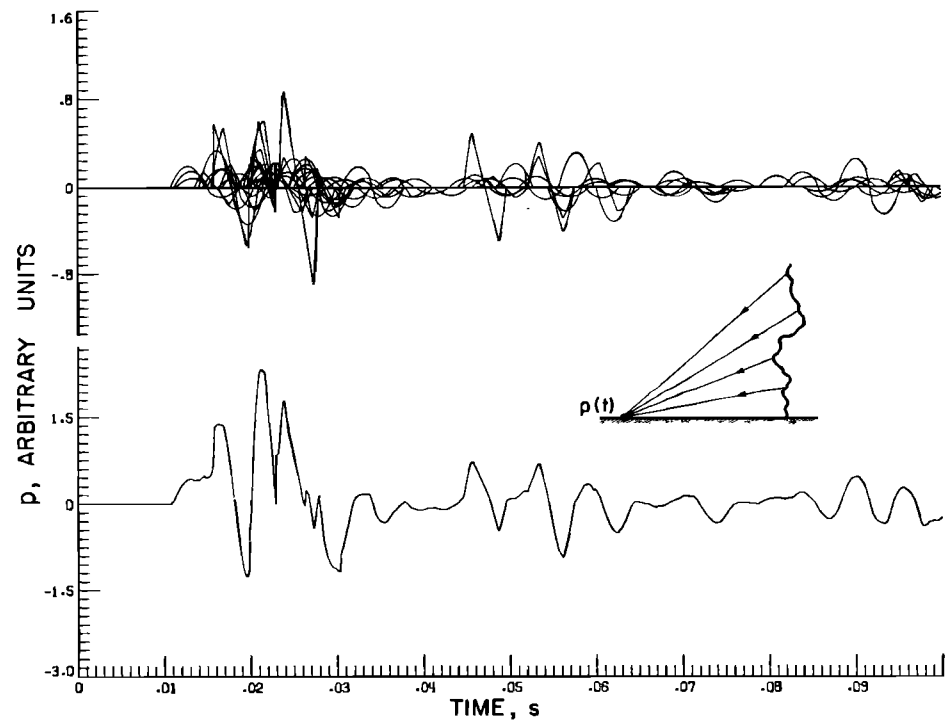

FIG. 12. (Top) Overlapping Wright–Medendorp waves received from individual segments of the "lightning" channel of Fig. 11. (Bottom) Resultant pressure-time history ("thunder" signature).

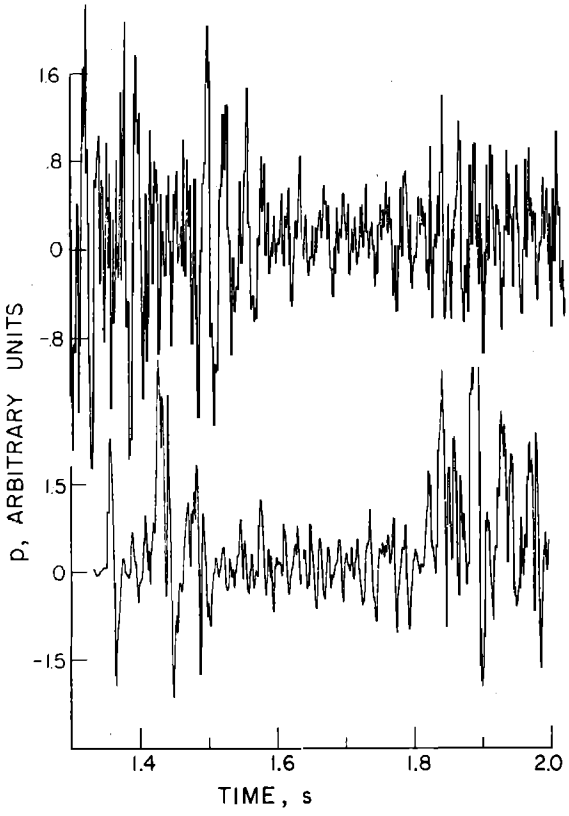

FIG. 13. (Top) 0.7-s signature segment of recorded real thunder.[26] (Bottom) Comparable segment of computer-generated thunder.

same tortuous channel. Thus there is a superposition of single-stroke thunder signatures, with appropriate time delays. In the computer plots one finds that former relatively quiet sections have now been filled in with peaks and valleys, so that the thunder is more continuous. However, otherwise the waveform doesn't appear qualitatively very different.

The computed thunder signature, Fig. 12, shows very marked variations along the time axis. These reflect corresponding marked variations in audible thunder: e.g., claps, rolls, and rumbles. Thus waveform comparisons must deal with similar features to avoid comparing "apples" with "oranges." Figure 13 shows a comparison on such a basis of a short segment of real thunder[26] (upper trace) and computer generated thunder from a triple-stroke flash (lower trace: from p_7 of Table I). The waveforms seem to be reasonably similar. Later we shall show spectral comparisons with real thunder.

Visual similarity of waveforms is subjective. A more exacting test—along with the later spectral comparisons—is afforded by the probability distribution of amplitudes. Figure 14 shows an overlay of amplitude histograms for samples of recorded real thunder[26] and of our computer thunder (p_1 to p_{16} of Table I repeated for a total of 102.4 s). The real thunder exhibits an essentially Gaussian probability density. The curve for the computer thunder, on the other hand, decays quasiexponentially from a peak or cusp at zero amplitude. Thus, relatively speaking, the computer thunder favors relatively low amplitudes in its distribution compared with real thunder. A tentative explanation is put forward in Sec. IVH.

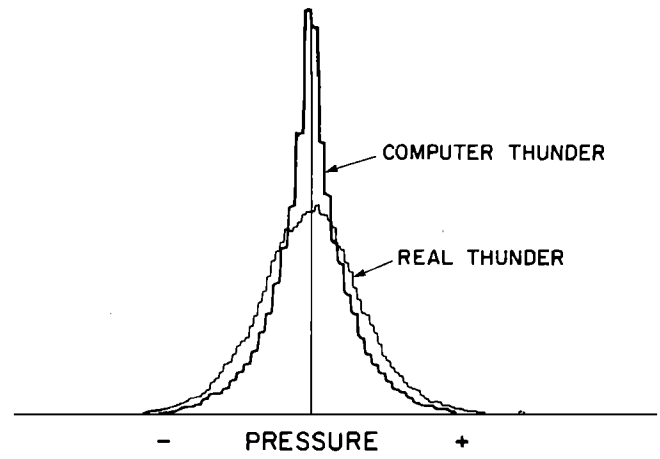

FIG. 14. Superposed histograms of signal amplitude distribution for computer-generated thunder and recorded real thunder.[26] (Arbitrary scale, but adjusted to comparable peak amplitude and area.)

B. Thunder signature convolves *N* wave with channel tortuosity

Thunder spectra are best understood when the signature in the time domain is portrayed as a convolution integral. Equation (1) may be thrown into such a form, provided the N wave stretching (growth in duration $2T$) is suppressed. Thus (with slight change in notation), (1) may be written as

$$p(t) = A \int N(ct - r)ds/r = A \int N(R - r)g(r)dr, \quad (14)$$

where

$$R = ct, \quad (15)$$

$$g(r) = \frac{1}{r}\frac{ds}{dr} = \frac{1}{r \sin \varphi}, \quad (16)$$

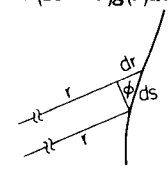

with T and A [cf., Eq. (2)] invariant with r. The integration is along the tortuous channel s.

Although the distance r from the observer is a unique function of distance s (measured, say, from the base of the channel), the converse is not true: $g(r)$ will be built up as a summation of single-valued parts along respective channel segments s_i:

$$p(t) = \sum_i p_i(t); \quad g(r) = \sum_i g_i(r), \quad (17)$$

$$p_i(t) = A \int_{s_i} N(R - r)g_i(r)dr. \quad (18)$$

Here each $p_i(t)$ is a uniquely defined convolution integral.

The Fourier transform of $p_i(t)$ with respect to R is

$$\hat{p}_i(k) = \frac{1}{2\pi} \int_{-\infty}^{\infty} p_i(t)e^{ikR}\, dR, \quad (19)$$

which yields the product of Fourier transforms, with a factor $2\pi A$:

$$\hat{p}_i(k) = 2\pi A \hat{N}(k)\hat{g}_i(k) \quad (20)$$

[defining $g_i(r) = 0$ for $r \neq r(s_i)$ so that the limits of (18) may be taken as $\pm \infty$]. It follows that

$$\hat{p}(k) = 2\pi A \hat{N}(k) \sum_i \hat{g}_i(k). \quad (21)$$

C. Tortuosity spectrum modulates *N*-wave spectrum

Equation (21) exhibits the *amplitude spectrum* $p(k)$ of the thunder as the product of two spectra: one is the Fourier transform $\hat{N}(k)$ of the basic N waves and the other is the Fourier transform of a function $\Sigma_i g_i(r)$ describing the tortuous lightning channel as viewed from the observer position. The respective *power spectra* are correspondingly related: a spectrum arising solely from the geometry of the lightning channel (as viewed by the observer, and hence specific to his location) multiplies or *modulates* the spectrum of the basic N wave to yield the thunder spectrum. Note that $k = \omega/c$ maps wavenumber spectra—appropriate to a spatial pattern such as the lightning channel—into frequency spectra. On this view, the spectral equation (21) is a consequence of the following fact: *the convolution equation* (14) *effectively maps the shape of lightning,* embodied in $g(r)$, *into the sound of thunder,* mediated by the "sonic boom" building blocks $N(ct - r)$.

Equation (21) may be evaluated for a tortuous lightning channel built up of rectilinear segments identified as the s_i. Then $p_i(t)$ is merely the Wright–Medendorp wave for the ith segment, given by Eq. (6). The Fourier transform is very simply evaluated, yielding the thunder amplitude spectrum as

$$\hat{p}(k) = A\hat{N}(k) \sum_i \frac{e^{jkr_i}}{\pi r_i} \frac{\sin[kl_i \sin \varphi_i]}{kc \sin \varphi_i}, \tag{22}$$

where

$$\hat{N}(k) = j\frac{2c}{T}\left(\frac{T}{kc}\cos \omega T - \frac{1}{k^2c^2}\sin \omega T\right) \tag{23}$$

is the N-wave spectrum. This may be converted from a spectrum in wavenumber k to one in radian frequency ω by means of the relations

$$\tilde{p}(\omega/c) = \hat{p}(k)/c; \quad k = \omega/c, \tag{24}$$

where $1/c$ is the Jacobian, $dk/d\omega$. [These correct the result, Eq. (8.2), obtained in a different fashion in Ref. 1, which lacks a factor $1/2\pi$.] Multiplying by the complex conjugate then yields the corresponding power spectrum. (It is argued in Ref. 1 that the cross spectra in the summation may be neglected.) Here again, in Eq. (22), the thunder spectrum is exhibited as the product of an N-wave spectrum and another arising from the channel tortuosity.

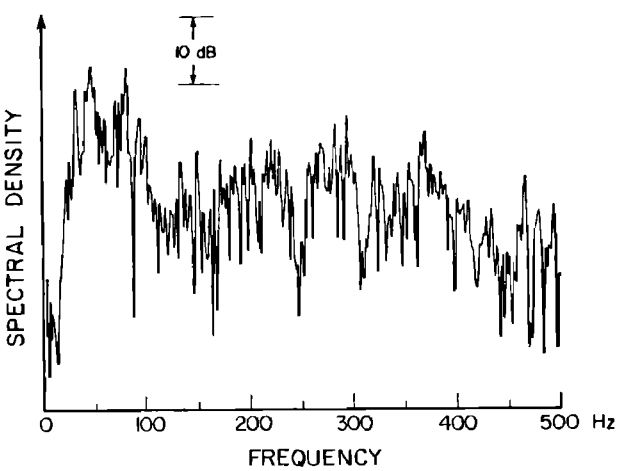

FIG. 15. Power spectrum of 0.8-s peal of real thunder.[26]

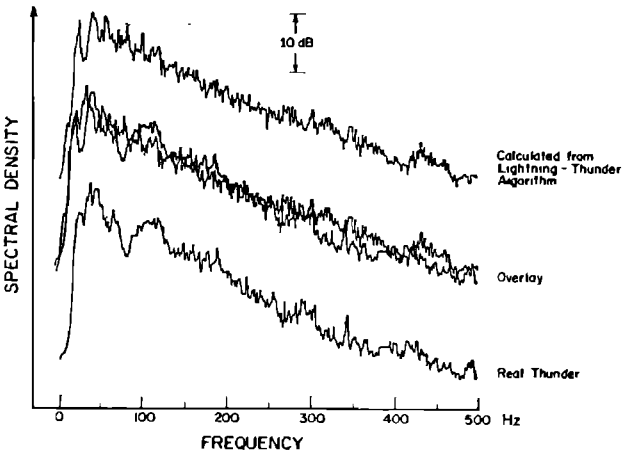

FIG. 16. Comparative 128-sample averages of 0.8-s power spectra. (Top) Computer-generated thunder. (Bottom) Segment of recorded real thunder.[26] (Middle) Overlay of the two spectra for comparison.

The channel tortuosity spectrum is as irregular in the frequency (or wavenumber) domain as the channel is in space. This irregularity in turn governs the features of thunder: e.g., the peals, rumbles, and rolls. Correspondingly, short term power spectra of thunder are as variable as the features they describe. We illustrate this in Fig. 15 with the power spectrum of an 0.8-s peal of recorded real thunder.[26]

Suppose, however, that we average successive 0.8-s thunder spectra for a minute or two: that is, over a succession of lightning strokes. Then the spectrum, whether for calculated or real thunder, will experience a considerable smoothing.

D. Smoothed spectra: Computed versus real thunder

Companion curves of smoothed spectra—computer-generated thunder (top) and recorded real thunder[26] (bottom)—are shown in Fig. 16, with shifted ordinate scales. Both were obtained via digital spectrum analyzer: 0.8-s spectra were averaged for 128 samples. In the middle is an overlay of the two spectra. Two further spectra of recorded real thunder,[26] obtained similarly, are overlaid in Fig. 17. Spec-

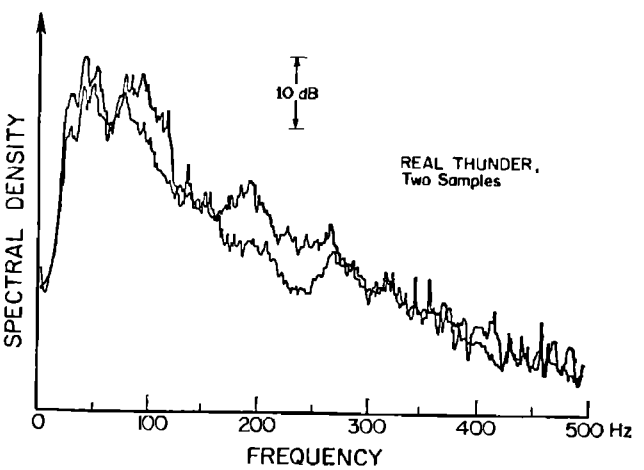

FIG. 17. Comparative 128-sample averages of 0.8-s power spectra: two further segments of recorded real thunder.[26]

trally, the computer thunder is seen to agree with samples of the real thunder about as well as they agree with each other.

The rather striking agreement of our examples of computer-generated and real thunder in Fig. 16 must be, in part, fortuitous. For one thing, published spectra of real thunder show considerable variability from one another (although much of this may be due to rather short averaging times, e.g., as in Ref. 27). For another, the computed thunder does not allow for either atmospheric attenuation or nonlinear waveform steepening: both can have significant effects on spectral shape, as discussed in Secs. IVG and H, respectively.

E. Spectral peak versus channel energy

We allude again to the thunder power spectrum, on our simplified theory, being a product of two spectra: the spectrum of the basic building blocks (here unstretched N waves), and the spectrum describing the channel tortuosity. The N-wave spectrum [cf., Eq. (23)] peaks at a frequency $f_p = 2/3T$, approximately. But the half-duration T of the N wave at a certain scaling distance (the cylindrical "relaxation radius"[7]) should be proportional to the square root of the energy/unit length E_l of the lightning stroke: this is inferred from the rigorous nonlinear theory of Plooster.[22] If the tortuosity spectrum were relatively flat near the N-wave spectral peak—a matter for speculation at present—then the latter would define the peak of the thunder spectrum. It follows that this would be diagnostic for inferring the specific energy E_l of the thunder stroke.

A similar conclusion concerning the spectral peak could be drawn if, instead of the N-wave shape, the basic building blocks were taken to have a somewhat different theoretically based waveform. In effect, this was done by Few[7] in pioneering this diagnostic role for the spectral peak. He used the waveform at 10 "relaxation radii" from a point explosion, taken from Brode's rigorous theoretical calculation[28]: the positive pulse resembles that of an N wave; the following negative pulse is rounded, lacking a terminal shock. *It is noteworthy that this early model overlooks the role of the tortuosity spectrum, in effect taking it to be flat.*

F. Spectral rolloff versus channel tortuosity

The asymptotic slopes on both sides of the spectral peak may also be diagnostic. Here, again, both the basic building blocks—N waves or other—and the channel tortuosity contribute. The respective spectral slopes (rolloffs) associated with the two-product spectra will add a log–log plot. Preliminary estimates already indicate that the tortuosity will likely increase the high-frequency rolloff by the order of 3 dB per octave: the amount will depend on the tortuosity statistics in conjunction with the basic segment lengths.

The N wave spectrum possesses zeros at the roots of $\omega T = \tan \omega T$. However, these do not appear in the thunder spectra of Figs. 16 and 17—either for calculated or real thunder. For the calculated spectrum of a single stroke the stretching of the N waves as they propagate will shift the zeros. The moderate shift may suffice to smear out the closely spaced zeros at the higher frequencies and reduce the first one to a dip. Multiple strokes—as on the computer thunder of Fig. 16—are more typical, and for these a further powerful smoothing effect is operative: this is the overlay of single-stroke spectra with the zeros markedly shifted to correspond to different N-wave durations. The combined effect appears to result in an absence of pronounced dips in the long term spectrum. [The calculation ignores the large stretching with reduced angle ϕ that is to be expected (Fig. 2). This is a still more powerful smoothing effect; it should also broaden the spectral peak.]

For various reasons we must regard N waves as oversimplified building blocks of real thunder. For the early part of the evolution, Brode[28] or Plooster[22] waveforms would seem more appropriate; these rounded waveforms with "tails" do not give rise to spectral zeros (Few,[7] Fig. 4).

G. Spectral rolloff versus atmospheric absorption

Atmospheric absorption from molecular relaxation will further accentuate the high-frequency rolloff,[29,30] as alluded to earlier. This will increase progressively with the observer distance from local segments of the lightning channel—hence, with time in the thunder record. It will also vary markedly with the temperature-humidity characteristics along the ray propagation paths.

The increase in rolloff is about 4 dB for the 200–400 Hz octave for an example worked out in Ref. 30: it refers to an intracloud flash with average propagation path (to the observer) characterized by 5 °C temperature, 80% relativity humidity, and 4-km length. Thus it would appear—very tentatively—that lightning tortuosity and atmospheric absorption may increase the high-frequency rolloff in dB by somewhat comparable, additive, amounts.

H. Spectral rolloff versus nonlinear waveform steepening

The present quasilinear theory of thunder generation completely lacks progressive nonlinear steepening of the pressure waves.[31] The initial steepening—front and rear shock waves—incorporated in the N-wave "building blocks" is an artifice that merely mimics part of the final effect. The N waves cannot evolve independently as we have postulated to justify linear superposition; rather it is the *resultant* waveform at any point that is progressively steepened during propagation, spoiling the independence. The final waveform $p(t)$ received by the observer will thus differ significantly in *local shape* from that calculated by summing N waves. (This is aside from any focusing/defocusing or scattering effects due to atmospheric wind/temperature gradients, or frequency-dependent atmospheric absorption.) Nevertheless, it does seem that the general *character* of the waveform pattern is correctly preserved (see Figs. 13 and 16).

As Pestorius and Blackstock[31] have pointed out, (i) the wave steepening will lead (or tend) to shocks; and (ii) small features on the $p(t)$ signature will be swallowed by the larger features or shocks, reducing the number of zero crossings. By Fourier analysis, (i) will add to the higher frequencies, whereas the longer wavelengths arising from (ii) will enhance the low frequencies. Thus the excluded nonlinear steepening would extend the spectrum at both ends.[31]

Stated differently, the nonlinear steepening would reduce the spectral rolloff rate with frequency at both ends. We note that this is opposite to the effect of atmospheric absorption at the high end: this may mitigate the error in our neglect of both. This nonlinear effect dominates the strong thunder near the channel where shock waves are evident. But farther out the atmospheric absorption diffuses the shocks to rounded shapes[32] and becomes a major factor in enhancing the high-frequency rolloff[29,30]; further nonlinear steepening is more than offset by the diffusion.

Item (ii) above may tend to explain the difference between the amplitude histograms of predicted and real thunder waveforms, Fig. 14. As mentioned earlier, the histograms show relatively *fewer* low-amplitude features in real thunder than in the linearized computer thunder. But the nonlinear steepening effective in real thunder is in the right direction to account for this: specifically, this is the tendency of the shocks to engulf low-amplitude features.

IV. CONCLUDING REMARKS

An approximate quasilinear theory of sound evolution from tortuous lightning channels has been developed herein. It has been shown to predict the major features of thunder deterministically,[33,34] with details of the rumble and roll. These cannot be accounted for by current theories that exclude the tortuosity but do allow for nonlinear effects.

Waveform distortion owing to the approximations is difficult to quantize; thus the credibility of our theory must depend on external evidence. We observe that the formalism is compatible with: (i) small scale experiments for sparks, and (ii) rigorous nonlinear analysis (to a point) for the specialized case of a rectilinear lightning channel. The predicted thunder (which can be heard via the bound-in soundsheet[35–37]) resembles real thunder in; (iii) waveform appearance, (iv) spectral characteristics, and (v) *audible sound*. It is further observed[35] that, by contrast, (vi) white noise filtered to a similar spectral shape does not mimic the sound of thunder. We emphasize that an approach to realism in the computer thunder is not an end in itself; it is, rather, one of several tests of the underlying physical model.

ACKNOWLEDGMENTS

We are grateful for the continued interest of a colleague, Professor Werner G. Richarz, and his assistance. He was instrumental in obtaining for comparison purposes some direct recordings of real thunder and the filtered white noise on the soundsheet; more importantly, he carried out the signal processing for Figs. 14–17. Support at the University of Toronto was aided by a grant from the Natural Sciences and Engineering Research Council of Canada, and at the NASA Langley Research Center, for one of us (HSR), by a period as Distinguished Research Associate.

[1]D. Roy, "A Monte Carlo Model of Tortuous Lightning and the Generation of Thunder," Univ. of Toronto Inst. for Aerospace Studies, Rep. 243 (CN ISSN 0082-5255) (1981).

[2]H. S. Ribner, Letter on computer model of thunder generation, and its audible demonstration, Sci. Am. **233** (3), 6 (March 1975).

[3]H. S. Ribner, F. Lam, K. A. Leung, D. Kurtz, and N. D. Ellis, "Computer Model of the Lightning→Thunder Process, with Audible Demonstration," AIAA Paper **75-548** (March 1975); also in *Progress in Aeronautics & Astronautics*, edited by I. R. Schwartz (AIAA Publication, 1976), Vol. 46.

[4]M. N. Plooster, "Numerical Model of the Return Stroke of the Lightning Discharge," Phys. Fluids **14**, 2124–2133 (1971).

[5]R. D. Hill, "Channel Heating in Return-Stroke Lightning," J. Geophys. Res. **76**, 637–645 (1971).

[6]"...human beings can recognize patterns in ways no contemporary computer can begin to approach," from F. H. C. Crick, Nobel laureate, "Thinking About the Brain," Sci. Am. (Sept. 1979).

[7]A. A. Few, "Power Spectrum of Thunder," J. Geophys. Res. **74** (28), 6926–6934 (Dec. 1969).

[8]A. A. Few, "Lightning Channel Reconstruction from Thunder Measurements," J. Geophys. Res. **75** (36), 7517–7523 (Dec. 1970).

[9]A. A. Few, "Thunder Signatures. EOS Transactions," Am. Geophys. Union **55** (5), 508–514 (May 1974).

[10]A. A. Few, "Thunder," Sci. Am. 80–90 and 132 (July 1975).

[11]D. R. MacGorman, A. A. Few, and T. L. Teer, "Layered Lightning Activity," J. Geophys. Res. **86** (C10), 9900–9910 (1981).

[12]A. A. Few and T. L. Teer, "The Accuracy of Acoustic Reconstruction of Lightning Channels," J. Geophys. Res. **79** (33), 5007–5011 (1974).

[13]The best resolution cited by Few and Teer[12] ($\pm$ 1/2° or $\pm$ 20 m at 2.5 km) presumably corresponds to *cross*-channel error. Resolution *along* the channel must be very much poorer, a $\frac{1}{4}$-s time average enveloping typically some 170 m at a ray angle of 30° with the horizontal. Such longitudinal error ($\pm$ 85 m) would be less easy to detect in comparisons[12] of channel reconstruction with photographs: it is primarily cross-channel error that would be noticeable.

[14]D. M. LeVine, "The Influence of Tortuosity on the Spectrum of Radiation from Lightning Return Strokes," Tech. Memo. 79544, NASA Goddard Space Flight Center (May 1978).

[15]D. M. LeVine and R. Meneghini, "Simulation of Radiation from Lightning Return Strokes: The Effects of Tortuosity," Radio Sci. **13** (5), 801–809 (Sept.–Oct. 1978).

[16]W. M. Wright and N. W. Medendorp, "Acoustic Radiation from a Finite Line Source with *N*-Wave Excitation," J. Acoust. Soc. Am. **43**, 966–971 (1968).

[17]The net effect at large distances (farfield) is as though *ds emitted* a wave of this form *ab initio*. Since this is a simpler concept and terminology, in what follows we will simply use the expression "emit" in place of "evolve nonlinearly."

[18]The duration $2T$ of the N wave should grow slowly with r by nonlinear stretching, with consequent reduction in A with r. This is neglected herein in figuring the emission from short lightning segments. But allowance is later made for the cumulative effect in the emission from a long tortuous channel.

[19]R. O. Onyeonwu, "Diffraction of Sonic Boom Past the Nominal Edge of the Corridor," J. Acoust. Soc. Am. **58**, 326–330 (1975).

[20]J. E. Piercy, T. F. W. Embleton, and L. C. Sutherland, "Review of Noise Propagation in the Atmosphere," J. Acoust. Soc. Am. **61**, 1403–1418 (1977).

[21]H. S. Ribner, M. E. Wang, and K. J. Leung, "Air Jet as Acoustic Lens or Waveguide," Proc. 7th International Congress on Acoustics, Budapest, 18–20 Aug. 1971, Vol. 4, 24 (9), 461–464 (1971).

[22]M. N. Plooster, "Shock Waves from Line Sources. Numerical Solutions and Experimental Measurements," Phys. Fluids **13**, 2665–2675 (1970).

[23]R. D. Hill, "Analysis of Irregular Paths of Lightning Channels," J. Geophys. Res. **73** (6), 1897–1906 (March 1968).

[24]L. D. Landau, "On Shock Waves at Large Distances from the Place of Their Origin," J. Phys. USSR **9**, 496–500 (1945).

[25]J. J. Gottlieb, "Simulation of a Travelling Sonic Boom in a Pyramidal Horn," in *Progress in Aerospace Sciences* (Pergamon, New York, 1976), Vol. 17, pp. 1–66 [see Eqs. (84) and (85)].

[26]W. G. Richarz and D. Roy, Unpublished tape recording of thunderstorm at University of Toronto Institute for Aerospace Studies, Toronto, Canada (15 July 1977).

[27]C. R. Holmes, M. Brook, P. Krehbiel, and R. McCrory, "On the Power Spectrum and Mechanism of Thunder," J. Geophys. Res. **76** (9), 2106–2115 (March 1971).

[28]H. L. Brode, "The Blast Wave in Air Resulting from a High Temperature, High Pressure Sphere of Air," Res. Mem. RM-1825-AEC, The Rand Corporation, Santa Monica, CA (1956).

[29]H. E. Bass and R. E. Losey, "Effect of Atmospheric Absorption on the

Acoustic Power Spectrum of Thunder," J. Acoust. Soc. Am. **57**, 822–823 (1975).

[30]H. E. Bass, "The Propagation of Thunder Through the Atmosphere," J. Acoust. Soc. Am. **67**, 1959–1966 (1980).

[31]F. M. Pestorius and D. T. Blackstock, "Propagation of Finite Amplitude Noise" in *Finite Amplitude Wave Effects in Fluids*, Proceedings of 1973 Symposium in Copenhagen, edited by L. Bjørnø (IPC Science and Technology, Guildford, England, 1974), pp. 24–29.

[32]P. L. Sachdev and R. Seebass, "Propagation of Spherical and Cylindrical *N*-waves," J. Fluid Mech. **58**, Part 1, 197–205 (1973).

[33]The rather similar notions of Professor Few[7–10] are potentially deterministic, but the format and predictions are qualitative. His ongoing studies have led to a comprehensive review article[34] that was received after the present paper was essentially complete. The two studies are complementary, with somewhat different treatment in areas of overlap. The difference is most marked in concepts governing the detailed waveform of the thunder signature.

[34]A. A. Few, "Acoustic Radiations from Lightning," *CRC Handbook of Atmospherics*, Vol. 2, edited by H. Volland (CRC Press, Boca Raton, FL, 1982), pp. 257–290.

[35]H. S. Ribner and D. Roy, *Computer Generated Thunder* (bound-in soundsheet). *Side 1.* Introduction. (i) Two minute sequence (with one exception) of triple-stroke computer thunder. Remarks. (ii) Shorter sequence of single-stroke computer thunder. *Side 2.* Remarks. (iii) Peals of computer thunder and real thunder[26] alternating for a total of six. Remarks. (iv) White noise filtered to simulate the spectral shape of thunder. Remarks. (v) Interval during a thunderstorm recorded in Toronto, 15 July 1977.[26]

[36]Specifics of the computer thunder signatures and filtered noise sequenced in (i) to (iv) of Ref. 35, identified in Table I. Sequence (i): triples, p_7, p_{10}, p_{13}, $p_{16}, p_7, \downarrow p_{16}\downarrow, p_7\downarrow, p_{27}\uparrow, p_{16}, p_7, p_{16}, p_{13}$, $\downarrow$ signifies recorded at low level, $\uparrow$, at high level. Sequence (ii): singles $p_1, p_2, p_8, p_9, p_{11}, p_{12}, p_{14}, p_{15}$. Sequence (iii): p_{10}, real thunder, p_{13}, real thunder, p_{27}, real thunder. Sequence (iv): white noise filtered to a spectral shape approximating the trend of Figs. 16 and 17.

[37]*Note added in proof*: As compared with the original tape recording, the soundsheet suffers from some nonlinear distortion of the louder thunder passages, with apparent amplitude reduction. This was a result of recording at a level high enough to yield acceptably low record surface noise at playback levels.